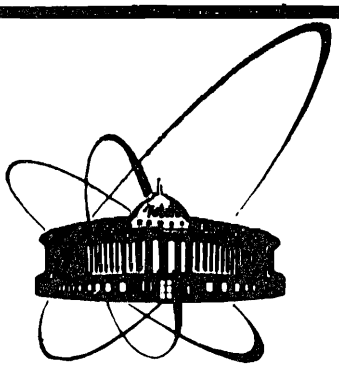

объединенный
институт
ядерных
исследований
дубна

E1-86-58

M.G.Dolidze, V.V.Glagolev, A.K.Kacharava*,
G.I.Lykasov, D.G.Mirianashvili*, M.S.Nioradze*,
Z.R.Salukvadze*, J.Urban

ENHANCEMENTS OBSERVED IN THE TWO-PROTON INVARIANT MASS DISTRIBUTION IN THE PIONLESS DEUTERON BREAKUP AT 3.3 GeV/c

Submitted to "Zeitschrift für Physik A"

* High Energy Physics Institute, Tbilisi

1986

Experimental Data

In the last few years in the two-nucleon systems produced in nucleon-nucleon and hadron-nucleon collisions new effects have been observed, which may be treated as dibaryon states. A search for such states is particularly interesting in connection with the predicted six-quark bags. Experimental results and their theoretical treatment have been already published in detail in a number of reviews, e.g., /1,2/. However, we should remark that not in all cases the resonance behaviour of the cross sections or of the two-nucleon effective mass distributions may be identified as a manifestation of dibaryon resonances /2/.

Using a 1m HBC exposed to beams of light nuclei /3/, such enhancements have been recently observed at 2.040 GeV/c^2 and 2.140 GeV/c^2. Besides, these peaks are observed in proton-proton combinations /4,7/ of the ^{4}Hep $\rightarrow$ dppn reaction, in proton-neutron /5/ combinations of the dp $\rightarrow$ ppn reaction and in neutron-neutron combinations of the dp $\rightarrow$ pπ^+nn reactions /6/.

In the effective masses of the pp-pair one of the peaks has been observed earlier /9/. The question arises whether such structures exist in proton-proton combinations of the dp $\rightarrow$ ppn reaction. It should be stressed that in all the quoted cases of the deuteron breakup only those events are taken into account which cannot be classified as quasi-nucleon ones, i.e., events without spectator nucleons. The ^{4}HeP $\rightarrow$ dppn reaction proceeds mainly via the mechanism in which two nucleons participate from ^{4}He and the remaining deuteron is a spectator /7/. The situation is quite different in the dp $\rightarrow$ ppn channel where quasi-elastic neutron-proton or proton-proton scattering takes place in the overwhelming majority of events. In this case the events, in which the momentum of the slowest nucleon ("spectator") in the deuteron rest frame is large enough, are conditionally regarded as spectatorless ones. Several cuts are taken as 300 MeV/c /6/ or 350 MeV/c /5/. If a cut is applied at too low momentum values, the hypothetical structure may be hidden due

to large quasi-elastic background. On the other hand, a cut in a too high limit improverishes statistics in the region of our interest.

In the following analysis we use the same experimental sample as in [5], namely, 20507 events of the dp → ppn reaction. All the values, if not stated explicitly, are given in the d rest frame.

One of the ways how to select spectatorless events may rise from the following considerations. Let us try to select the class of inelastic scattering, e.g., with virtual π^- -meson production and absorption [9,10]. Due to kinematical constraints on π^- -meson absorption with a single nucleon, the majority of these events occurs on a nucleon pair. Figure 1 shows a plot of the effective mass of two slow nucleons versus four-momentum transfer squared from the incident proton to the leading particle for the charge retention channel. In our terminology charge retention and charge exchange channels mean a leading proton and neutron in the final state, respectively. It can be seen that the events are extensively grouped according to the quasi-elastic nucleon-nucleon kinematics. An analogous plot in the dp → pppπ^- channel is demonstrated in Fig. 2.

It should be noted that from the kinematic constraint for the quantities put on the axes x and y such a plot reflects only the incident proton momentum loss. Supposing that in the dp → ppn channel the produced π^- -meson is almost on-mass-shell, the comparison of these two plots allows us to select the sample of wanted events. They will lie above the line presented in figs. 1 and 2. Such a procedure is also applied to the charge exchange channel. The momentum distributions of the slowest nucleon from the selected groups of events are presented in figs. 3a and 3b for the charge retention and charge exchange channels, respectively. In the momentum distribution of the slowest nucleon in the charge retention channel two maxima are seen (fig. 3a) which split up at about 200 MeV/c. The first of them corresponds to a part of quasi-elastic NN scattering and the second maximum to the events with π^- -meson absorption.

Previous studies of the dp → ppn reaction at 3.3 GeV/c have proved that the high momentum tail in the charge exchange channel substantially exceeds that of the charge retention one [9]. This phenomenon has been explained taking the corresponding isospin states into account by contributions of inelastic processes such as Δ° -isobar exchange or virtual π^- -meson production and absorption [8-11]. To attract the above mechanisms have been also

Fig. 1. Slow proton and neutron effective mass versus four-momentum transfer squared - from incident proton to leading one - for the charge retention part of the dp → ppn reaction.

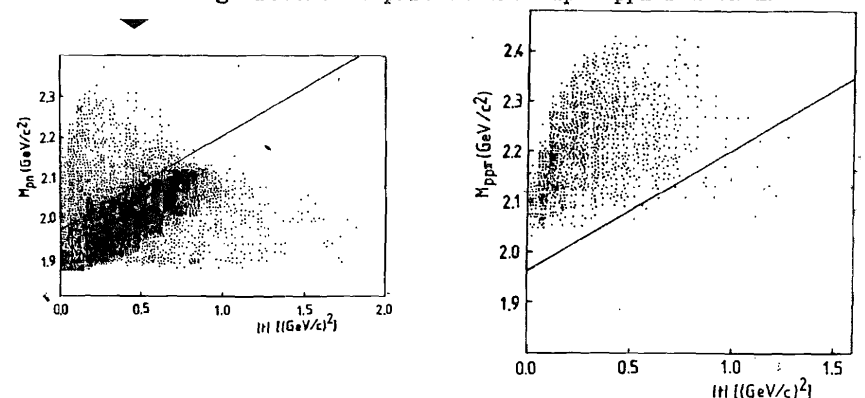

Fig. 2. pp·π^- effective mass, without the leading proton, versus four-momentum transfer - from incident proton to leading one - for the dp → pppπ^- reaction.

Fig. 3. Momentum distribution of the slowest nucleon in the deuteron rest frame: for the charge retention (————) and charge exchange (- - - -) channels. The events are taken from the "pion absorption region".

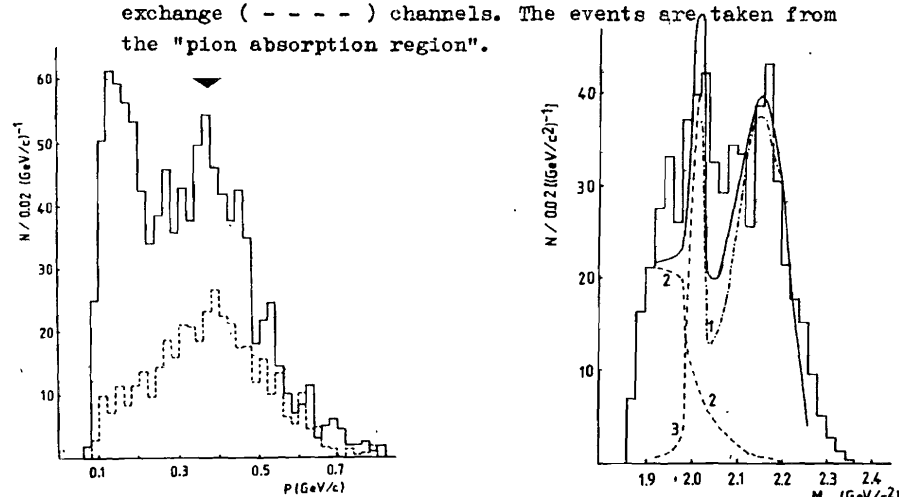

Fig. 4. Two-proton effective mass distribution from the charge exchange channel for both protons with momenta over 200 MeV/c: histogram - experimental results, full curve - calculated result. Curves 1 and 3 correspond to the diagrams 6a and 8a, respectively. Curve 2 corresponds to elementary p-n charge exchange.

necessary in the analysis of ^{4}Hep→dppn at 8.6 GeV/c[7]. If one also takes into account a relatively big slope of the np charge exchange differential cross section it is not surprising that the second maximum preponderates over the first one in the slowest proton momentum distribution of the charge exchange channel (fig. 3b).

Applying the cut at p = 200 MeV/c for the slowest nucleon momentum, the effective mass distribution of the two protons is histogrammed for the charge exchange channel. The result is shown in fig. 4. Two maxima can be seen approximately at the same masses as in pn and nn combinations [5,6].

The fit of a second order polynomial background and two Breit-Wigner functions to the experimental distribution gives the values of maxima and widths displayed in table 1[13]. The table summarizes the results of other papers as well.

Table 1. Review of two-nucleon effective mass enhancements

Reaction	Reference	M_1 MeV/c^2	Γ_1 MeV/c^2	C_1	M_2 MeV/c^2	Γ_2 MeV/c^2	C_2
^{4}Hep→dppn	/4/	2035±15	30±23	4.1	2137±15	59±20	5.1
dp→(pn)p	/5/	2020±10	45±20	4.3	2130±10	20±10	4.5
dp→(pp)n	/13/	2014±10	63±28	4.0	2162±10	18±26	4.4
dp→ppπ^+(nn)	/6/	2035±20	50±20	5.0	2143±20	60±20	5.0
π^- ^{12}C→(pp)+x	/14/	2016±3	30±14	4.4	-	-	-
π^- ^{12}C→(pp)+x	/15/	2017±1.3	5±2	3.4	-	-	-
pd→p(pn)	/16/	-	-	-	~2140	~30	-

C_1, C_2 are the ratios of the excess over the background to the square root of the background. The errors of masses M_1 and M_2[4,5,13,6] are the mass resolution of the chamber.

Cut at 350 MeV/c is applied in ref.[5]. This choice is justified whereas the admixture of quasi-elastic events to the charge retention channel at p = 200 MeV/c is fairly large as shown in fig. 3a.

The authors of ref.[12] have observed no enhancements. This is connected with the following fact: the effective mass distribution M_{pn} contains both np combinations in the charge retention part of the dp → ppn reaction, and in the charge exchange channel, the statistics for the M_{pp} distribution becomes insufficient, because of a high value of the applied cut.

Moreover, in ref.[12] the missing mass methodical cut is applied to the reaction as a whole whereas the nature of missing mass distributions in the charge retention and charge exchange channels is quite different. The same distributions from our results are shown in fig. 5, the arrows indicate the cut limits applied in [12]. It is easy to see that such a cut rejects 20% of events in the charge retention channel and 56% of events in the charge exchange one. In this way more than half of the events from the charge exchange channel is lost, and a natural ratio of the charge retention and charge exchange deuteron breakup cross sections is deformed.

As is seen from table 1, nowadays quite enough experimental material is available about the enhancements in two-nucleon effective masses over the range under study.

2. Discussion of the Results

The resonance behaviour of the effective mass distribution of two protons suggests the question if they can be treated as an evidence for dibaryon resonances.

The effective mass squared distribution $S_2 \equiv M_{pp}^2$ of the two protons in the dp → ppn reaction is written as:

$$\frac{d\sigma}{dS_2} = \frac{1}{4M_d|\vec{p}_0|^2(2\pi)^5}\int\frac{d^3\vec{p}_1\,d^3\vec{p}_{23}}{2E_1\,2E_{23}}\,\delta^4(p_0+p_d-p_1-p_{23})\int\frac{d^3\vec{p}_2\,d^3\vec{p}_3}{2E_2\,2E_3}\,\delta^4(p_2+p_3-p_{23})|F_d|^2. \qquad (1)$$

Here the following notations are used: M_d is the deuteron mass, P_0, P_d, P_1, P_2, P_3 are the four-momenta of the incoming proton, deuteron and outgoing neutron and two protons, respectively; $\vec{P}_0$, $\vec{P}_1$, $\vec{P}_2$, $\vec{P}_3$ are their three-momenta; E_1, E_2, E_3 are the energies of the outgoing nucleons; $\vec{P}_{23}$, E_{23} are the sum of three-momenta and energies of two final protons, respectively, F_d is the reaction amplitude. The dp → ppn reaction, in principle, may proceed via virtual π-meson production in the intermediate state and its further absorption.

The main contribution to the analysed distribution comes from

the diagrams illustrated in figs. 6-8. The diagrams in figs. 6 and 7 show one pion exchange and single pn and pp scatterings, respectively; the triangular diagrams with one pion exchange are given in fig. 8. It should be noted that the diagrams in fig. 8a,b may be reduced to the diagrams in fig. 6, if vertices Γ_1 and Γ_2 are presented as a one pion exchange diagram. For convenience we divide the contributions from the diagrams in figs. 6 and 8, i.e., for $M_{pp} < 2.02$ GeV/c^2 we use the contribution from the triangular diagrams of fig. 8, and for $M_{pp} \geq 2.02$ GeV/c^2 the contribution from the diagrams of fig. 6.

A detailed analysis of the diagrams 6-8 has been carried out in /17/. For this reason only the final expressions for their contributions to the investigated M_{pp} distribution will be presented.

After standard calculations the matrix element squared for one pion exchange can be written as:

$$|F_d^{(1)}|^2 = \frac{g^2 t\, G_1(t)}{(t+\mu^2)^2} \left| f^{off}_{\pi d \to NN} \right|^2 , \qquad (2)$$

where $g^2/4\pi = 14.7$.

$t = (P_0 - P_1)^2$

μ is the mass of the real π-meson,

$G_1(t)$ is the off-energy-shell π-meson formfactor,

$f^{off}_{\pi d \to NN}$ is the amplitude of virtual pion absorption by the deuteron.

So to turn to the real π-meson in the π d $\to$ NN amplitude in expression (2), the results of /18,19/ are used. Taking into account different normalizations of the amplitudes, one can get:

$$f^{off}_{\pi d \to NN} = G_2(q^{off}, q^{on}) (q^{off}/q^{on})^{\frac{1}{2}} f^{on}_{\pi d \to NN} , \qquad (3)$$

where "off" and "on" denote the off-energy-shell and on-energy-shell π-mesons, respectively; q is the pion momentum in the π-d CMS. Substituting (3) into expression (2) and $|F_d^{(1)}|^2$ into (1), one obtains the one pion exchange contribution of fig. 6a,b to the M_{pp} distribution of the dp $\to$ pnn reaction:

$$\frac{d\sigma^{(1)}}{dM_{pp}} = \frac{g^2 M_{pp}^2}{8\pi^2 M_d^2 |\vec{p}_0|^2} \int_{t_{min}}^{t_{max}} \frac{q^{off}\, \sigma_{\pi^+ d \to pp}(E_\pi(t, M_{pp}))}{(t+\mu^2)^2} G_2^2(q^{off}, q^{on})\, t\, G_1(t)\, dt , \qquad (4)$$

where $\sigma_{\pi^+ d \to pp}(E_\pi(t, M_{pp}))$ is the cross section of the real π^+d $\to$ pp process as a function of pion energy, which, in its turn, depends on the 4-momentum transfer squared t in the upper vertex of the

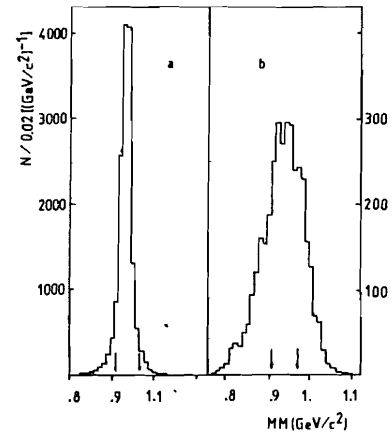

Fig. 5. Missing mass distribution for the dp $\to$ ppn reaction:
a) charge retention channel,
b) charge exchange channel.

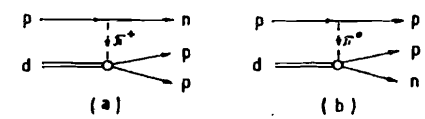

Fig. 6. One pion exchange diagrams.

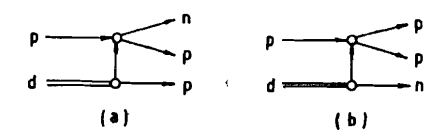

Fig. 7. Single pn and pp scattering diagrams.

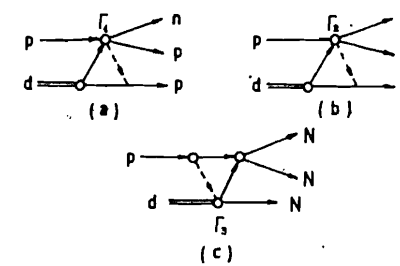

Fig. 8. Triangular diagrams with one pion exchange.

diagram in fig. 6a and on the effective mass of the two final protons. The formfactors $G_1(t)$ and $G_2(q^{off}, q^{on})$ are taken from /18,19,20/.

As known, the cross section of the π^+d $\to$ pp process is of the resonance-like form as a function of the pion energy E or as a function of the two proton invariant mass at $E_\pi \simeq 0.26$ GeV or $M_{pp} \simeq 2.16$ GeV /21/. This behaviour is due to the fact that the process mainly proceeds via intermediate Δ^{++} production at the above pion energy /21,22/. At $E_\pi = 0.14$ GeV, what corresponds to a real pion kinetic energy of several MeV, or $M_{pp} \simeq 2.02$ GeV/c^2 in the $\sigma_{\pi^+ d \to pp}$ cross section a narrow peak some MeV in width has been predicted theoretically /23/ according to the $1/v = E_\pi / q^{on}$ law, where v is the pion velocity, and to the Coulomb repulsion at $v \to 0$.

As stated above, the intermediate pion on the diagram of fig. 6a is off-energy-shell, and its momentum is expressed in terms of the invariant mass M_{pp} and transfer t as:

$$q^{off} = \left\{ \left[(M_{pp}^2 - M_d^2)/2\sqrt{s} \right]^2 - t \right\}^{\frac{1}{2}},$$

which shows that for $M_{pp} = 2.02$ GeV/c^2 $q^{off} \neq 0$. In this connection, because the integral expression (4) contains the product of q^{off} and the cross section of the real $\pi^+ d \to pp$ process, a peak in the $\sigma_{\pi^+ d \to pp}(E_\pi(t, M_{pp}))$ cross section at $M_{pp} = 2.02$ will manifest itself in the $d\sigma^{(1)}/dM_{pp}$ distribution of the $dp \to ppn$ reaction. We remark that if the intermediate pion in fig. 6 were a real one, i.e. if it were on-energy-shell then no peak would be observed in $d\sigma^{(1)}/dM_{pp}$ at $M_{pp} = 2.02$ GeV/c^2, as seen from (4). In other words, as it follows from (3) /18,19/, the off-energy-shell amplitude of the $\pi d \to NN$ process must contain a peculiarity of the $1/\sqrt{q^{on}}$ type (see (3)) at $q^{on} \to 0$ so that the one pion exchange diagram in fig. 6 might reproduce the peak in the M_{pp} distribution of the $dp \to ppn$ reaction at $M_{pp} = 2.02$ GeV/c^2

The calculation of $d\sigma^{(1)}/dM_{pp}$ by the formula (4) shows that the peak at $M_{pp} = 2.02$ GeV/c^2 is wider than the predicted one /23/ and the width of the second peak is approximately the same as that of the $\pi^+ d \to pp$ process at $M_{pp} = 2.16$ GeV/c^2.

The diagram shown in fig. 6b gives a similar resonance-like contribution to the proton-neutron effective mass distribution. Its contribution to M_{pp} is negligible in comparison with that of the diagram in fig. 6a as the evaluation shows. This is particularly evident when the neutron is the fastest of the three final nucleons. The resonance-like behaviour of the two proton invariant mass distribution is experimentally observed only in this case. We remark that taking into account the vector meson exchange diagrams does not affect the result qualitatively. And to take account of them quantitatively is too complicated.

The contribution $d\sigma^{(2)}/dM_{pp}$, corresponding to the diagram of fig. 7a, to the M_{pp} distribution of the reaction under study is of the following form /17/:

$$\frac{d\sigma^{(2)}}{dM_{pp}} = M_{pp}\, m^2 \int \frac{d\sigma_{pn}^{c.e}}{dt} |\Phi_0(p_3)|^2 \frac{p_3 d\Omega_3 dt}{E_2 E_{23}}, \qquad (5)$$

where $d\sigma_{pn}^{c.e}/dt$ is the pn charge exchange differential cross section, Ω_3 is the proton solid angle in the lower vertex diagram in fig. 7a, m is the nucleon mass.

A similar expression can be obtained for the contribution of the diagram in fig. 7b, $d\sigma^{(2)}/dM_{pn}$; to the proton-neutron invariant mass distribution changing correspondingly the neutron for the proton. The contribution of the diagram in fig. 7b to the two-proton invariant mass distribution, M_{pp}, is overwhelmed by that of the diagram in fig. 7a because the neutron is the fastest nucleon in the final state, so it can neglected.

The contribution, $d\sigma^{(3)}/dM_{pp}$, of the triangular diagram, corresponding to fig. 8a, is of the following form /17/:

$$\frac{d\sigma^{(3)}}{dM_{pp}} = \frac{g^2 M_{pp} |F_\pi|^2}{16\pi} |I_1|^2 \int \frac{q^2 E(q)}{E_2(E_2+E_3)|\vec{p}_3|^2} \left\{ \int \frac{d\sigma_{pp\to np\pi^+}}{dT_2\, d\Omega_2 d\Omega_1} + \right.$$

$$\left. + 2 \left(\frac{d\sigma_{pp\to np\pi^+}}{dT_2 d\Omega_2 d\Omega_1} \cdot \frac{d\sigma_{pn\to pn\pi^0}}{dT_2 d\Omega_2 d\Omega_1} \right)^{\frac{1}{2}} + \frac{d\sigma_{pn\to pn\pi^0}}{dT_2 d\Omega_2 d\Omega_1} \right\} d\Omega_2 d\Omega_1, \qquad (6)$$

where $I_1 = \int_0^\infty \exp(i\alpha x)\, \phi_0(x)\, dx$ and ϕ_0 is the deuteron ground-state wave function, $\alpha = (E_N(p_3) - E_\pi(p_3) - m) E_\pi(p_3)/p_3$, $d\sigma_{NN\to NN\pi}/dT_2 d\Omega_2 d\Omega_1$ is the differential cross section of the $pp \to pn\pi^+$ and $pn \to pn\pi^0$ reactions.

When evaluating the expression (6), the differential cross sections $d\sigma_{NN\to NN\pi}/dT_2 d\Omega_2 d\Omega_1$ have been calculated in the approximation of one meson reggeized exchange /24/.

The calculations show that the contribution of the diagram in fig. 8b to the M_{pp} distribution of the reaction studied is negligibly small as the final neutron is fast and it mainly comes from the upper vertex and not from the lower one (see figs. 8a,b). The contribution from the diagram of fig. 8c is also small so that it is of the second order in comparison with the diagrams of figs. 8a or 6a. Since the final neutron is fast, the probability of its formation in the first collision of the incident proton with the nucleon in the deuteron is higher than in the $\pi d \to NN$ process (see fig. 6a) or after the $NN \to NN$ rescattering (see fig. 8c). A detailed analysis of the diagrams in figs. 8b,c has been carried out in paper /25/, where it is shown that their contributions to the spectrum of protons flying into the backward hemisphere is negligible for the $dp \to ppn$ reaction. Because we deal here with the M_{pp} distribution of the above reaction in the same kinematical region as in /25/, the diagrams in figs. 8b,c are not taken into account.

We remark that the rescattering of the incident proton after the p-n charge exchange (see fig. 7a) on the proton from the deuteron also makes a small contribution to the M_{pp} distribution of the reaction in question. A detailed discussion can be found in /25/. So this small contribution is also neglected.

A final expression for the M_{pp} distribution of the discussed $dp \to ppn$ reaction can be written as the sum of the diagrams in figs. 6-8 taking into account

$$\frac{d\sigma}{dM_{pp}} = \frac{d\sigma^{(1)}}{dM_{pp}} + \frac{d\sigma^{(2)}}{dM_{pp}} + \frac{d\sigma^{(3)}}{dM_{pp}} + \frac{d\sigma^{(inter)}}{dM_{pp}}, \qquad (7)$$

where $d\sigma^{(inter)}/dM_{pp}$ is the contribution of the interference of the digrams in figs. 6a,7a,8a, the way of their calculation is taken from /17/.

Main contributions to the proton-neutron invariant mass of the $dp \to ppn$ charge retantion reaction come from diagrams in figs. 6b, 7b,8b.

Figure 4 displays the results of calculations corresponding to the contributions of the diagrams in figs. 6a,7a,8a and their sum to the $d\sigma/dM_{pp}$ distribution according to the formulae (1)-(7). One can see a qualitative agreement between the calculated and experimental M_{pp} distributions /13/. Moreover, the figure also shows that character of the distribution is mainly determined by the one pion exchange diagram of fig. 6a. The other diagrams only touch up the resonance-like form of the spectrum.

Thus, the observed enhancements in the two proton invariant mass at $M_{pp} \simeq 2.02$ GeV/c^2 and $M_{pp} \simeq 2.16$ GeV/c^2 from the $dp \to ppn$ /13/ reaction are mainly determined by virtual pion absorption on the deuteron. But as indicated above, for the peak at $M_{pp} \simeq 2.02$ GeV/c^2 one has to assume an irregularity in the off-energy-shell pion absorption amplitude by the deuteron out of the physical region near a zero momentum of the real pion ($q^{on} = 0$). This behaviour of the off-mass-shell amplitude $f_{\pi d \to NN}$ seems to be due to the existence of two-nucleon quasibound states. The same conclusion is valid for the character of the proton-neutron invariant mass distribution where irregularities are observed approximately at the same M_{pn} values /5/. The diagram in fig. 5b, the π^- meson exchange, again makes a main contribution to the M_{pn} distribution.

The behaviour of the M_{nn} distribution in the more complicated $dp \to p\pi^+nn$ reaction may be similar to the above described one, as observed experimentally /6/. From the theoretical point of view it is most convenient to calculate the two-proton invariant mass distribution in the $dp \to ppn$ reaction because the $\sigma_{\pi^+ d \to pp}$ behaviour is well-known over a wide range of π^+-meson energy. So the quantitative calculations have been carried out in this paper for the above case.

Now we are going to discuss the consequence that follows from the analysis of the one pion exchange of fig. 6a for the cross section ratio $R = \frac{\sigma_{pp}}{\sigma_{cE}} / \frac{\sigma_{pn}}{\sigma_{ch.r.}}$ of a pp pair in the charge exchange and an np pair in the charge retention channels of the $dp \to ppn$ reaction for different areas of invariant masses. At $M_{NN} \simeq 2.02$ GeV/c^2 the diagrams in figs. 6a and 6b differ from one another mainly by coupling constants g_{π^+} and g_{π^0} in the upper vertices, respectively, as the $\pi^+ d \to pp$ and $\pi^0 d \to pn$ cross sections at very small pion momenta behaves similarly, like 1/v. Because of $g_{\pi^+} = \sqrt{2}\, g_{\pi^0}$, the contributions of the diagrams in figs. 6a and 6b at $M_{NN} \simeq 2.02$ GeV/c^2 yield $R = 2$. At $M_{NN} \simeq 2.16$ GeV/c^2 the $\pi^+ d \to pp$ and $\pi^0 d \to pn$ processes in the lower vertices (figs. 6a and 6b) proceed via Δ^{++} and Δ^0 productions, respectively; the isospin ratio gives $R \simeq 3$. These values of R at $M_{pp} \simeq 2.02$ GeV/c^2 and $M_{NN} \simeq 2.16$ GeV/c^2 agree quite well with the experimental data (see table 2).

Table 2

Contribution	σ_{tot} (mb)	σ_1^{exp} (μb)	σ_2^{exp} (μb)	R_1^{exp}	R_1^{th}	R_2^{exp}	R_2^{th}
pn	30.8±1.2	200±20	85±15	1.9±0.4	2.0	4.1±1.1	3.0
pp	6.4±0.2	76±12	69±11				

Assuming that the small shift in the positions of the pp and pn invariant mass maxima is caused by the methodics, the last result may serve as an additional confirmation of the conclusion that the intermediate pion absorption by the deuteron is likely to be the basic reason of the resonance-like behaviour of the two-proton invariant mass in the reaction under study.

Conclusion

In this paper it is shown that at a certain cut applied to the slow proton momenta of the $dp \to ppn$ reaction a similar structure can be observed in the two proton invariant mass distribution as

in those of pn and nn combinations. Two maxima have been observed at 2.02 GeV/c^2 and 2.16 GeV/c^2. The observed effect is assumed to be caused mainly by virtual pion absorption on the deuteron. Besides, the existence of the peak at $M_{NN} \approx$ 2.02 GeV/c^2 requires the presence of some irregularity in the behaviour of the off-energy-shell $\pi d \to NN$ reaction amplitude near the threshold.

References

1. Yokosawa A., Proceedings of the Meeting on Two-Nucleon Systems and Dibaryon Resonances, Hiroshima, Japan 1979,ANL-HEP-CP-80-81; Phys.Rep. 64, 47(1980).
2. Makarov M.M., Sov.Phys.Usp. 136, 185(1982).
3. Aladashvili B.S. et al., Nucl.Instr.Methods 129, 109(1975).
4. Glagolev V.V. et al., JINR Report, E1-83-59, Dubna, 1983; Z.Phys. A 317, 334(1984).
5. Siemiarczuk T. et al., Phys.Lett. 128B, 367(1983).
6. Siemiarczuk T. et al., Phys.Lett. 137B, 434(1984).
7. Zielinski P. et al., Sov.Nucl.Phys. 40, 482(1984).
8. Poster R. et al., Phys.Lett., 33, 1625(1974).
9. Aladashvili B.S. et al., Nucl.Phys. A274, 186(1976).
10. Glagolev V.V. et al., JINR Report, 1-84-519,Dubna, 1984.
11. Aladashvili B.S. et al., Nucl.Phys. B86, 461(1975).
12. Katayama N. et al., Nucl.Phys. A423, 410(1984).
13. Glagolev V.V. et al., JINR Rapid Comm. 5, 13(1984).
14. Bayramov A.A. et al., JINR Report, P1-83-207, Dubna, 1983.
15. Azimov S.A. et al., Preprint, 27-84-FVE, Tashkent, 1984.
16. Andreev V.P. et al., LIYAF, M1011, Leningrad, 1984.
17. Dolidze M.G. et al., JINR Report, P2-84-831, Dubna, 1984.
18. Landau R.H., Thomas A.V., Nucl.Phys. A302, 461(1978).
19. Thomas A.W., Nucl.Phys. A258, 417(1976).
20. Mescheryakov M.G. et al., Dokl.Akad.Nauk. 100, 677(1955); Nuovo Cimento Suppl. 3, 120(1956). Barry George W.W., Ann.Phys. 73, 482(1972).
21. Richard-Serre C. et al., Nucl.Phys. B20, 413(1970).
22. Brack M. et al., Nucl.Phys. A287, 425(1977).
23. Gell-Mann M., Watson K., Ann.Rev.Nucl.Science 4, 219(1954).
24. Ponomarev L.A., Physics & Nuclei 7, 186(1976).
25. Amelin N.S., Lykasov G.I., Sov.Nucl.Phys. 28, 1258(1978).

Received by Publishing Department
on January 31, 1986.

Долидзе М.Г.

E1-86-58

Наблюдение особенностей в спектре эффективных масс двух протонов в безмезонном развале дейтрона при 3,3 ГэВ/с

Анализируются неспектаторные события безмезонного развала дейтрона при импульсе 3,3 ГэВ/с, полученные на 100 см водородной пузырьковой камере ЛВЭ ОИЯИ. Наблюдены максимумы при значениях 2010 и 2160 МэВ/c^2 в спектрах эффективных масс двух протонов из реакции перезарядки. Проведены теоретические расчеты, учитывающие диаграммы однопионного обмена с поглощением виртуального π-мезона дейтроном. Показано, что пик при M_{pp}= 2010 МэВ/c^2 может быть объяснен только при наличии особенности в поведении внеэнергетической амплитуды реакции $\pi^+ d \to pp$ вблизи порога. Наблюдаемый пик при M_{pp} = = 2160 МэВ/c^2 обусловлен, в основном, образованием Δ-изобары в промежуточном состоянии при поглощении π-мезона дейтроном.

Работа выполнена в Лаборатории высоких энергий ОИЯИ.

Препринт Объединенного института ядерных исследований. Дубна 1986

Dolidze M.G.,

E1-86-58

Enhancements Observed in the Two-Proton Invariant Mass Distribution in the Pionless Deuteron Breakup at 3.3 GeV/c

A sample of "non-spectator" events in the pionless deuteron breakup at a 3.3 GeV/c momentum has been investigated by means of a 1 m HBC at JINR, Dubna. The two-proton invariant mass spectrum in the charge exchange channel exhibits two enhancements for masses of 2010 MeV/c^2 and 2160 MeV/c^2. Theoretical calculations taking into account one-pion exchange diagrams and virtual pion absorption by the deuteron have been carried out. It has been shown that the enhancement at M_{pp}= 2010 MeV/c^2 can be explained if there is an irregularity in the behaviour of the off-energy-shell amplitude of the $\pi^+ d \to pp$ reaction near the threshold. The observed maximum at M_{pp}= 2160 MeV/c^2 is caused mainly by intermediate Δ production and pion absorption on the deuteron.

The investigation has been performed at the Laboratory of High Energies, JINR.

Preprint of the Joint Institute for Nuclear Research. Dubna 1986